OXFORD

The surgical destabilization of the abductor muscle leads to development of instability-associated hip osteoarthritis in mice

Michael B. Geary[1,4], Caitlin A. Orner[1,4], Helen Shammas[1,2], John M. Reuter[1],
Alayna E. Loiselle[1,3], Brian D. Giordano ®[1,3,5] and Chia-Lung Wu ®[1,3,5*]

[1]Center for Musculoskeletal Research, University of Rochester Medical Center, 601 Elmwood, Avenue, Box 665, Rochester, NY 14642, USA,
[2]Department of Biomedical Engineering, University of Rochester Medical Center, 601 Elmwood Avenue, Box 665, Rochester, NY 14642, USA and
[3]Department of Orthopaedics and Rehabilitation, University of Rochester Medical Center, 601 Elmwood Avenue, Box 665, Rochester, NY 14642, USA

[4]Co-first authors.
[5]Co-last authors.

*Correspondence to: C.-L. Wu. E-mail: Chia-lung_Wu@urmc.rochester.edu

ABSTRACT

Osteoarthritis (OA) of the hip is a common and debilitating painful joint disease. However, there is paucity of surgically induced hip OA models in small animals that allow scientists to study the onset and progression of the disease. A growing body of evidence indicates a positive association between periarticular myotendinous pathology and the development of hip OA. Thus, in the current study, we aimed to establish a novel mouse instability–associated hip OA model via selective injury of the abductor complex around the hip joint. C57BL6/J mice were randomized to sham surgery or abductor injury, in which the myotendinous insertion at the third trochanter and greater trochanter were surgically detached. Mice were allowed free active movement until they were sacrificed at either 3 weeks or 20 weeks post-injury. Histologic analyses and immunohistochemical staining of the femoral head articular cartilage were performed, along with microCT (μCT) analysis to assess subchondral bone remodeling. We observed that mice receiving abductor injury exhibited significantly increased instability-associated OA severity with loss of proteoglycan and type II collagen staining compared to sham control mice at 20 weeks post-surgery, while comparable matrix metalloproteinase 13 expression was observed between injury and sham groups. No significant differences in subchondral bone remodeling were found after 3 or 20 weeks following injury. Our study further supports the link between abductor dysfunction and the development of instability-associated hip OA. Importantly, this novel surgically induced hip OA mouse model may provide a valuable tool for future investigations into the pathogenesis and treatment of hip OA.

INTRODUCTION

Osteoarthritis (OA) affects over 32.5 million people in the United States, and approximately 10% of adults over the age of 45 years will suffer from symptomatic hip OA at some point in their life [1]. The hip is a diarthrodial joint that permits multidirectional range of motion, and it is the second most commonly OA-affected large joint, after the knee [2]. Hip OA is generally divided into primary idiopathic and secondary causes. Secondary degeneration of the hip has been associated with a number of identifiable factors including obesity, pathomorphologies such as femoral acetabular impingement [3] and structural hip instability due to acetabular dysplasia, trauma, or musculotendinous dysfunction [4]. Despite significant investigation into causative factors of hip OA, the underlying etiology remains elusive.

Dynamic stability of the hip is maintained by the periarticular muscles of the joint, in particular, the gluteus medius and minimus and their associated tendons. It is well-recognized that altered arthrokinematics affects articular cartilage loading and can contribute to the progression of OA [5–8]. Indeed, multiple studies have observed an association between periarticular tendinopathy and hip OA [9, 10]. For example, patients with severe abductor tears demonstrated a high rate of concomitant intra-articular injury [11]. These studies provide a compelling rationale for developing an animal instability-associated hip OA model by inducing muscular injury surrounding the hip joint.

Animal models used to investigate the pathogenesis of hip joint OA mostly utilize large animals such as canines [12–14], sheep [15] and pigs [16]. Selection of these larger animal models offers the advantage of similar cartilage morphology, thickness and injury response as seen in humans [17–19]. The existing large animal hip OA models not only provide us invaluable insights into hip cartilage physiology and pathophysiology but

also serve as essential preclinical models for drug development. Despite these benefits, large animals are not amenable to genetic modification to better define the cellular and molecular mechanisms of pathogenesis, as can be conducted in mice [19]. Furthermore, there is a paucity of literature on murine hip injury models [20]. The purpose of the present study was to establish a novel murine model of instability-associated hip OA induced by abductor injury. We hypothesize that a surgically induced abductor injury can lead to the development of hip OA in mice. The OA severity, subchondral bone remodeling, and anabolic and catabolic biomarkers were evaluated by histology, immunohistochemistry (IHC) and microCT (μCT) analyses in the current study.

MATERIALS AND METHODS
Mouse hip OA model of abductor instability

All animal procedures were approved by the University Committee on Animal Research at the University of Rochester. All mice were maintained under pathogen-free conditions in the vivarium at the University of Rochester. Not more than five animals were housed per cage, and all mice were housed under standardized light–dark cycle conditions with controlled temperature and humidity. Female C57BL/6J mice (8- to 10-weeks-old; #00664, Jackson Laboratories; Bar Harbor, ME) weighing on average between 20 and 25 g were anesthetized by intraperitoneal injection of ketamine (60 mg/kg) and xylazine (4 mg/kg). The hind region and right leg were shaved and prepared with alcohol and betadine (povidone-iodine). The proximal femur was approached through a 1-cm lateral skin incision placed over the third trochanter (3T), followed by a direct incision through the fascial layer, exposing the underlying third and greater trochanters (GTs).

Mice were randomly divided into two groups. One group underwent surgically induced abductor injury, while the other group received sham surgery. The effect of abductor injury on hip OA development was investigated at two time points following surgery: 3 and 20 weeks post-surgery. Four or five mice per group (sham or surgery) were included per time point. The sham group underwent anesthesia along with incisions of the skin and fascia. A schematic diagram of the right proximal femur shows the locations of the femoral head (FH), GT, lesser trochanter (LT), 3T and sciatic nerve (SN) (Fig. 1A). Coronal μCT reconstruction of the right hip demonstrates the anatomic positions of the FH and GT (Fig. 1B). The 3T is visible with a needle placed into the muscular attachments. The insertion of gluteus maximus at 3T (Fig. 1C) and muscular attachments of the large abductor complex (ABD, including gluteus medius, gluteus minimus, and tensor fascia latae) from the GT (Fig. 1D) were cut in this injury model. During each surgery, careful attention was paid to avoid injury to the SN running posterior to the proximal femur. For all mice, the fascial layer was closed with a single 5-0 nylon suture (Ethicon, Inc.), and the skin was closed with either 7 mm stainless steel wound clips (CellPoint Scientific Inc., Gaithersburg, MD) or a series of interrupted 5-0 nylon sutures. For analgesia, mice were given subcutaneous buprenorphine (0.05 mg/kg) at the time of surgery and on each subsequent day for the next 72 hours. Following surgery, mice were returned to their cages and allowed free active motion, feeding (i.e. *ad libitum*) and weight bearing. No special accommodations were required post-surgery. Animals were monitored daily until they were sacrificed.

Evaluation of bone tomography

Mice were sacrificed at either 3 or 20 weeks post-surgery (*n* = 4–5 per group per time point). Immediately after sacrifice, the hemi-pelvis and femur were prepared by removing the skin and excess soft tissue, leaving the hip and the major muscular attachments around the pelvis and femur. The samples were fixed for 72 h in 10% neutral buffered formalin, then washed with PBS, placed in 70% EtOH and subjected to the μCT scanning. Hips were scanned using the VivaCT 40 system (Scanco Medical, Basserdorf, Switzerland) at highest resolution with a pixel size of 10.5 μm to image bone. An integration time of 300 ms and an X-ray voltage of 55 kVP were used. The hip was captured and segmented using a scanning threshold of 320 to identify bone. The FH was analyzed for trabecular bone (excluding cortical bone) at a threshold of 310. Views of the FH and acetabulum were analyzed using a threshold of 320. The Gaussian method was used for noise reduction (sigma 0.8 with a support value of 1 pixel).

Evaluation of OA severity

Following 72 h of fixation and μCT scanning, samples were decalcified in 14% EDTA (pH 7.2) at room temperature for 2 weeks. Samples were then dehydrated and embedded in paraffin with the posterior surface of the hip facing down. Using the SN as a landmark, serial sections (thickness = 5 μm) were taken through the preserved hip and surrounding soft tissue in a coronal plane. Three different levels were cut through the joint, with five sections taken at each level.

Safranin O/Fast Green staining was used to visualize changes in the hip articular structure and proteoglycan content at 3 and 20 weeks post-surgery. Slides were baked overnight at 60°C, then deparaffinized and rehydrated via graded ethanol solutions. After air drying, slides were stained in Weigert's Hematoxylin for 7 min (equal parts Solution A, CAS# 517-23-2 and Solution B, CAS# 7705-08-0) and then rinsed with running tap water. Slides were stained with 0.02% Fast Green (CAS# 2353-45-9) for 3 min, rinsed with 1% acetic acid for 10 s and then stained with 1% Safranin O (CAS# 477-23-6) for 5 min. After a quick rinse with 0.5% acetic acid and double-distilled water, slides were then air-dried and cover-slipped.

OA severity was determined by the modified Mankin scoring system as previously described [21]. Briefly, three independent blinded graders assessed sections for degenerative changes in the hip articular cartilage. Scores including articular structure (0–11), tidemark (0–3), loss of proteoglycan staining (0–8) and chondrocyte clones (0–2) were averaged among graders for the hip FH, resulting in total scores between 0 and 24.

IHC

IHC was performed for collagen Type II A1 (COL2A1) and matrix metalloproteinase 13 (MMP13). For both protocols, slides were baked overnight at 60°C, then deparaffinized and rehydrated through graded ethanol solutions. IHC labeling for MMP13 began with enzymatic antigen retrieval using hyaluronidase (Sigma-Aldrich, St. Louis, MO; H-3506) for 10 min in a 37°C water bath. Endogenous peroxidase was then quenched for 30 min using endogenous blocking reagent (Dako
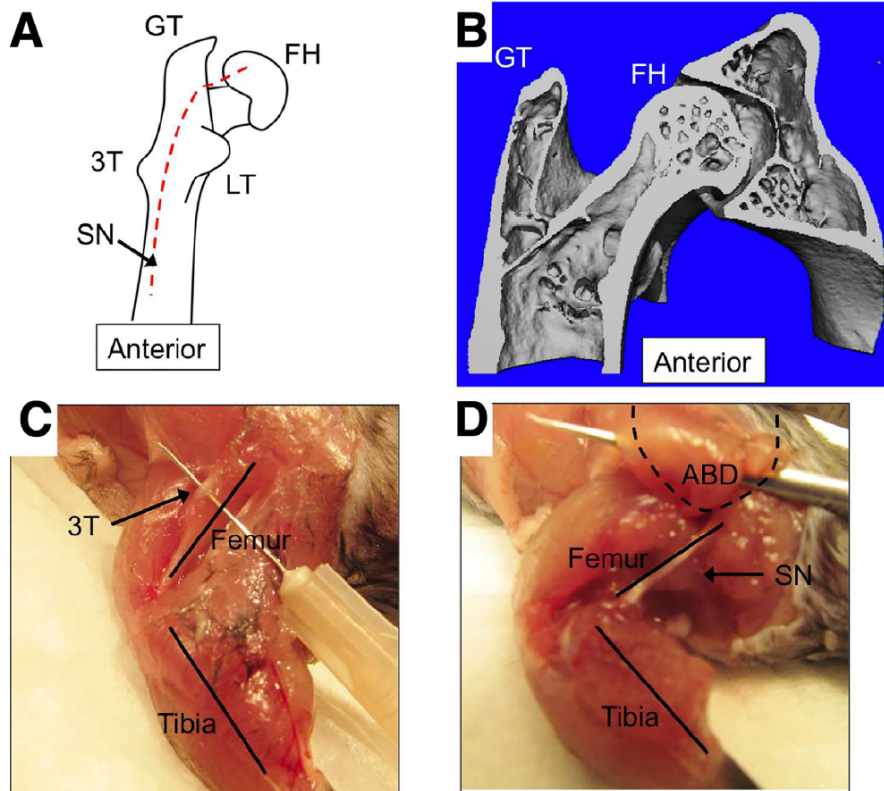
Fig. 1. Surgical model of abductor complex injury. (A) Schematic of the right proximal femur showing the locations of the FH, GT, LT and 3T, as well as the path of the SN running posterior to the femur. (B) Coronal reconstruction of the right hip showing the anatomic positions of the FH and GT. (C) Photograph of the left hind limb with skin removed. The femur and tibia are labeled for orientation. The 3T is visible superficially, with a needle placed into the muscular attachments. Attachments running proximal from the 3T were cut in this injury model. (D) Photograph of the left hind limb highlighting the abductor complex (ABD) to the GT (dashed outline). The entire abductor complex was cut in the injury group. The femur, tibia and SN are labeled for orientation. FH: femoral head; GT: greater trochanter; LT: lesser trochanter, 3T: the third trochanter; SN: sciatic nerve; ABD: abductor complex.

North America, Carpinteria, CA; S2003). After rinsing with deionized water and phosphate-buffered saline containing 0.1 % Tween-20, slides were blocked for 30 min with 5% Normal Horse Serum (NHS; Vectastain Elite ABC Kit, Mouse IgG, Vector Laboratories, Burlingame, CA; PK-6102) followed by the Blocking Endogenous Antibody Technology kit (Invitrogen Corporation, Camarillo, CA; 50-300). Overnight incubation with the MMP13 primary antibody (Thermo Fischer Scientific, Waltham, MA; MS-825P; 1:200 dilution) was conducted at 4°C with control slides incubated with mouse IgG at the same concentration (1 μg/ml). On the second day, sections were incubated with the secondary antibody (Vector PK-6102) followed by avidin-biotin complex (ABC reagent; Vector PK-6102). Color was detected using the Vector DAB ImmPACT kit (Vector SK-4105) counterstained with hematoxylin.

IHC labeling for COL2A1 was performed as follows. Enzymatic antigen retrieval was performed for 10 min in a 37°C water bath using pepsin (Sigma-Aldrich, P7000). After rinses, sections were blocked with endogenous blocking reagent (Dako, S2003) for 30 min followed by 5% NHS (Vector PK-6102) for 30 min. The COL2A1 primary antibody (Thermo Scientific, MS235-P; 1:100 dilution) was left to incubate at 4°C overnight with control slides incubated with the same concentration of mouse IgG (2 μg/ml). On the second day, sections were incubated with the secondary antibody (Vector PK-6102) and ABC reagent (Vector PK-6102). Color was then detected with the Vector DAB ImmPACT kit (Vector SK-4105) counterstained with hematoxylin.

The COL2A1 IHC was quantified based on an previously reported method [22]. In brief, the areas of uncalcified cartilage of the hip FHs were selected as regions of interest (ROIs) by the freehand drawing tool in Fiji (https://imagej.net/software/fiji/downloads). Selected ROIs were then added to the ROI manager, duplicated and converted into 8-bit images. The threshold was set at 0 and 160 for minimum and maximum values for all images. 'Area' and 'Limit to threshold' were selected in the 'Set Measurements' tab under the 'Analyze' menu. The results of %area were compared between mice receiving Sham and Abductor surgery.

The MMP13 IHC was quantified by counting the cells that were positive for MMP13 staining due to its low matrix staining intensity. Proprietary methods were used according to the Fiji plugin 'Cell Counter' (https://imagej.nih.gov/ij/plugins/cell-counter.html). 'Cell Counter' can be found in 'Plugins' in the 'Analyze' menu. The results of %MMP13 cells in uncalcified cartilage areas were compared between mice receiving Sham and Abductor surgery.

Statistics

To determine how surgery, time (following surgery) and their interaction (surgery × time) affected hip OA severity and subchondral bone remodeling, data were analyzed by two-way repeated measures analysis of variance (ANOVA) followed by Sidak's multiple comparisons test ($\alpha = 0.05$) using GraphPad Prism version 9. Values are expressed as mean ± SD.

RESULTS

Mice receiving abductor surgery demonstrated significantly increased instability-associated hip OA severity compared to the sham group 20 weeks following injury

Safranin O is a cationic dye that stains proteoglycans, and the intensity of red Safranin O staining is a proxy for proteoglycan content. Loss of proteoglycan content is a clinical hallmark of OA [23]. Hips from the sham and injured groups were stained at 3 and 20 weeks post-injury with Safranin O/Fast Green to visualize proteoglycans. Twenty weeks after injury, mice in the surgery group demonstrated loss of proteoglycan staining of the uncalcified articular relative to the sham group, although the structure of the articular cartilage surface was comparable between the two groups (Fig. 2A and B, yellow arrows). No significant difference in OA severity was observed between sham and injured groups at 3 weeks post-injury. In addition, sham mice had similar OA severity at 3 and 20 weeks post-surgery. Note that both sham mice and injured mice at 3 weeks post-surgery (i.e., around 11–13 weeks of age) still exhibited remaining physes (black arrows) under the articular cartilage as mice are known to complete epiphyseal fusion at 15 weeks of age [24].

Mice receiving abductor surgery exhibited decreased COL2A1 staining but comparable MMP13 staining in the articular cartilage relative to sham mice at 20 weeks following abductor injury

IHC labeling for COL2A1 and MMP13 in articular cartilage of the FH was performed at 20 weeks post-injury as this was the time point when OA was evident in the mice that
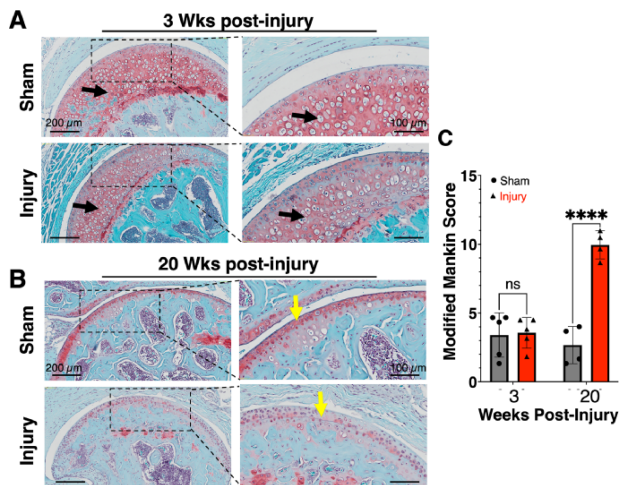

Fig. 2. Abductor injury results in loss of proteoglycan staining 20 weeks post-surgery. Coronal sections through the hip were stained with Safranin O/Fast Green, in which proteoglycan stains red. Staining with increased magnification is shown for sham and injured groups at (A) 3 weeks and (B) 20 weeks after surgery. Loss of proteoglycan staining in the uncalcified cartilage is evident in the injured group after 20 weeks relative to the sham group. Black arrows: growth plate cartilage. Yellow arrow: articular cartilage. (C) Modified Mankin scores show increased OA severity of the mice receiving surgery 20 weeks post-injury as compared to the corresponding sham group. Two-way repeated measures ANOVA followed by Sidak's multiple comparisons test. **** $P < 0.0001$. Mean $\pm$ SD. Abbreviation: ns: not statistically significant.

received surgery. In the sham group, a superficial layer of uncalcified cartilage was characterized by pericellular staining of COL2A1 (Fig. 3A). In the deeper layers, staining intensity was increased and more evenly distributed throughout the extracellular matrix. Semi-quantification of COL2A1 IHC showed that mice with abductor injury had significantly decreased COL2A1 staining in the uncalcified cartilage compared with mice in the sham group. MMP13 has been shown to play a catabolic role in OA [25], and increased staining of MMP13 has been observed in animal models of arthritis [26, 27]. IHC staining for MMP13 was performed to visualize changes in FH articular cartilage after sham surgery and abductor injury. There was no appreciable staining for MMP13 in the articular cartilage at 20 weeks post-injury in either the sham or surgery group (Fig. 3B).

μCT reveals no significant change in subchondral bone parameters 20 weeks post-injury

To evaluate potential structural changes in subchondral bone, hips from the sham group and the injury group were analyzed by μCT to compare subchondral microtrabecular volumetric parameters 3 and 20 weeks following injury (Fig. 4). No significant changes in cancellous bone fraction (bone volume/total volume; BV/TV, excluding the cortex) were detected in the injured group relative to sham at 20 weeks (sham: 0.51 ± 0.1; injury: 0.51 ± 0.1) (Fig. 4A). In addition, there were no significant differences in trabecular bone characteristics between the two groups. This includes trabecular number (sham: 6.3/mm $\pm$ 0.8; injury: 6.3/mm $\pm$ 0.4) (Fig. 4B), trabecular thickness (sham: 79.2 μm $\pm$ 8.1; injury: 81.8 μm $\pm$ 7.3) (Fig. 4C) and trabecular spacing (sham: 151.8 μm $\pm$ 23.5; injury: 147.5 μm $\pm$ 10.8) (Fig. 4D).

DISCUSSION

Currently, only a few rodent hip OA models have been established. These models can be generally categorized as either chemically or surgically induced OA [20, 28]. Intra-articular injection of monosodium iodoacetate (a chondrocyte glycolytic inhibitor) triggered rapid hip OA development compared to controls within 14 days in a rat model. However, it is not clear whether such a progressive and destructive OA phenotype represents chronic human hip OA. In another study, various degrees of hip instability—mild, moderate, severe and FH resection—were surgically induced in mice at weaning (3-weeks-old neonatal pups) [20]. These data suggest that progressive hip instability resulting from periarticular soft tissue insufficiency led to morphometric changes in the growing mouse hip. However, the direct relationship between abductor injury and hip OA in mice with mature pelvic bone structure (i.e. complete fusion of triradiate cartilage; 8- to 10-week-old) was unknown [29]. Here, our study demonstrated the feasibility of surgical destabilization of abductor muscles, leading to the development of instability-associated hip OA in mice. Furthermore, this small animal hip OA model may be used to explore the sequence of pathoanatomical and anabolic/catabolic effects on OA onset and progression due to severe tendon injuries.

Reliable animal models of surgically induced OA require technical steps that can be easily followed and reproduced [17]. In this model, the 3T serves as a surgical landmark, which can be palpated before making the skin incision. Once the muscular
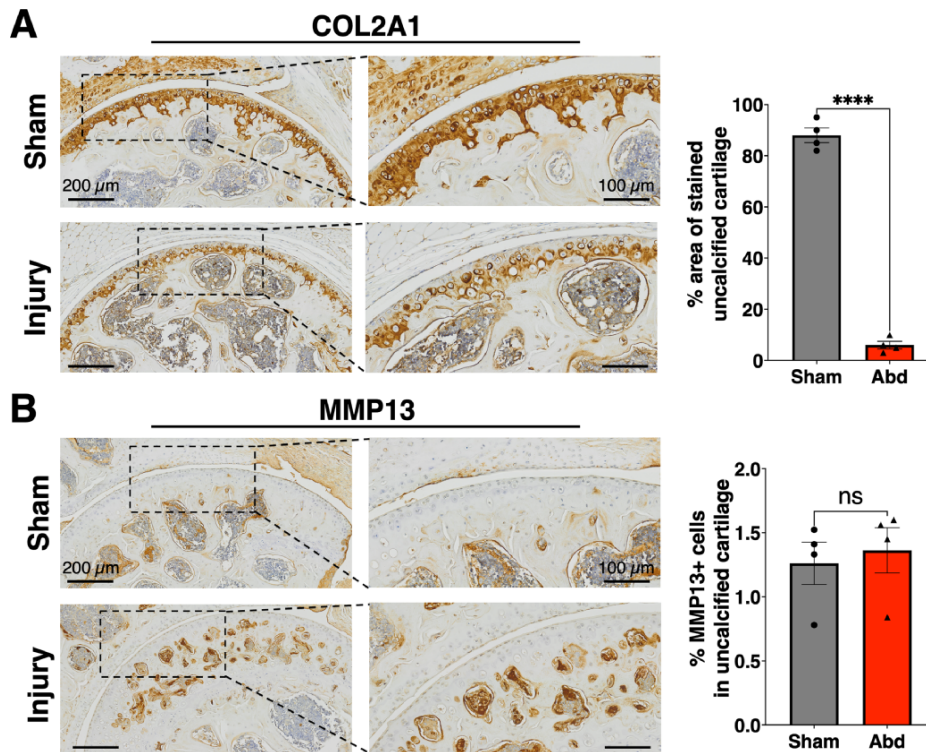
Fig. 3. COL2A1 and MMP13 staining reveal loss of type II collagen content in the uncalcified hip cartilage of the mice 20 weeks post-surgery. Coronal sections through the hip are shown following IHC for (A) COL2A1 and (B) MMP13 staining with semi-quantification using Fiji. Brown color indicates positive staining. Significantly decreased COL2A1 staining was observed in the uncalcified hip cartilage of the mice receiving surgery; however, no apparent staining for MMP13 was detected in either the sham or surgery group. **** $P < 0.0001$. Mean $\pm$ SD. Abbreviation: ns: not statistically significant.

attachments to the 3T have been cut, the femur is followed proximally to the large ABD on the GT. These muscles are easily visualized and can be cleanly dissected without injuring surrounding structures. This surgical method also avoids dissecting deep tissues and the SN running posterior to the proximal femur. In preliminary work, we experimented with performing a capsulotomy to induce more severe injury. Through multiple surgeries, we found that the joint capsule was too small to be reliably incised without damaging the SN, which runs closely to the joint. Thus, mice with capsulotomies have been excluded from the present work.

The primary findings in this study were the loss of proteoglycan and COL2A1 staining (hallmarks of OA) in uncalcified articular cartilage 20 weeks after injury, indicating abductor injury successfully induced hip cartilage degeneration. Additionally, the observation that sham mice had similar OA severity 3 and 20 weeks after surgery suggests that both sham surgery and aging (i.e., ~6 months of age) were not sufficient to induce hip OA. We also observed that abductor injury did not affect epiphyseal fusion, which is generally completed by 15 weeks of age in mice [24]. Remarkably, no changes in MMP13 IHC staining were observed between the sham and injured groups, suggesting that either MMP13 may not be the main catabolic mediator in our mouse hip OA model or other time points may need to be investigated to establish a temporal expression pattern of MMP13 in instability-associated hip OA. Our results are consistent with the findings from the study by Killian et al., in which the authors

demonstrated low MMP13 staining in articular cartilage in their titrated model of hip dysplasia [20]. Future studies investigating other cartilage degradation enzymes—such as a disintegrin-like and metalloproteinase with thrombospondin motif (ADAMTS) family, MMP3 and MMP9—and additional time points post-surgery are warranted. Radiographic analysis of subchondral bone remodeling did not reveal significant differences between sham and injured groups at any time point investigated in this study. Nevertheless, long-term study with *in vivo* μCT analysis may be required to observe subchondral bone remodeling in our mouse model.

The gluteus medius and minimus, in conjunction with the tensor fascia latae and gluteus maximus, represent the main components of the hip abductor complex. This complex contributes to the 'contractile layer' of the hip and is thought to exert considerable influence on the intra-articular joint space and its associated layers [30]. In a clinical outcome study that evaluated the results of arthroscopic gluteus medius/minimus repairs, a high incidence of concomitant intra-articular hip pathology was noted [11]. Abductor tendon pathology leads to considerable pain and functional impairment. Both open and arthroscopic repair techniques have been proposed, and excellent clinical results have been reported for both repair types [11, 31, 32]. The positive relationship between periarticular myotendinous pathology, including hip abductor diseases, and progression of OA has been suggested [9, 33–35]. For example, a recent study examining the ultrastructure of the abductor tendon complex in patients
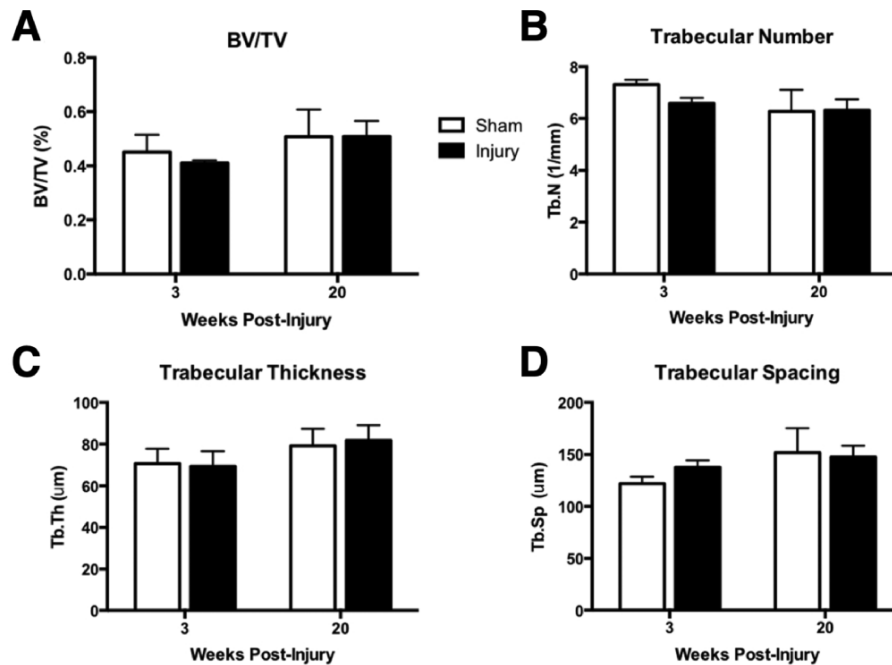
Fig. 4. µCT analysis indicates no significant changes in subchondral bone parameters following abductor injury. µCT was used to assess the subchondral bone of the FH. (A) BV/TV, (B) trabecular number, (C) trabecular thickness and (D) trabecular spacing were measured at 3 and 20 weeks post-surgery for both sham and surgery groups. There were no significant differences in subchondral bone parameters between the two groups at any time point investigated. Two-way repeated measures ANOVA followed by Sidak's multiple comparisons test. Mean ± SD.

treated for either femoral neck fractures or OA (total hip arthroplasty) indicated that all OA patients had coexisting tendinosis, with greater degenerative changes and scarring than the patients with traumatic fractures [10]. It is likely that abductor compromise, through an analogous pathomechanical process, contributes to the onset and progression of instability-associated hip OA. Therefore, re-establishment of an effective abductor force coupling mechanism may help optimize and rebalance joint loading, reducing the progression of cartilage degeneration that may ultimately result in the need for joint arthroplasty.

While our present study establishes a reproducible injury-induced mouse hip OA model and offers an important step forward in investigating the role of abductor insufficiency in the development of hip OA, there are limitations that must be considered. First, the mechanisms underlying abductor insufficiency leading to mouse hip OA development remain to be determined. In particular, the effects of abductor surgery on both biomechanical loading of hip cartilage and mouse behaviors such as pain, gait, and weight bearing need to be quantified. Second, our surgical procedure produces major injuries that are much more severe than those described in human subjects with typical tendinopathies. Hence, the current instability-associated hip OA model may not completely recapitulate the natural development of primary OA in humans as post-traumatic OA generally exhibits relatively rapid disease progression compared to primary OA [36]. Third, the clinical relevance of a quadruped model for hip OA and potential biomechanical differences compared to human bipedal locomotion must be considered. Specifically, whether the abductor muscles are used similarly in humans and quadrupeds warrants further investigation, although mice and humans share similar joint congruence at the hip. Finally, only female mice were used in the current work. Our rationale for this was based on the increased incidence and progression rate of hip OA in women versus men as described by several studies [37–39]. Despite these limitations, we demonstrated that destabilization of abductor muscles leads to the development of instability-associated hip OA in mice.

In conclusion, we have established a novel murine model of instability-associated hip OA through an injury to the abductor complex around the hip. This model may be utilized as a valuable tool to examine potential biomarkers associated with hip OA progression, particularly in patients with severe tendon injuries [40]. We believe that for the broader orthopedic community of clinicians and researchers, our findings will increase understanding of the role of abductors in hip stability and the development of joint pathology.

DATA AVAILABILITY

The data that support the findings of this study are available from the corresponding author upon reasonable request.

ACKNOWLEDGEMENTS

assistance in performing modified Mankin score grading for hip joint OA severity for the current project.

FUNDING

CONFLICT OF INTEREST STATEMENT

B.D.G is a consultant to Arthrex Inc. and receive royalties and research support from Arthrex Inc.

AUTHOR CONTRIBUTIONS

REFERENCES

1. Lawrence RC, Felson DT, Helmick CG *et al.* Estimates of the prevalence of arthritis and other rheumatic conditions in the United States: part II. *Arthritis Rheum* 2008; **58**: 26–35.

2. Zhang W, Moskowitz RW, Nuki G *et al.* OARSI recommendations for the management of hip and knee osteoarthritis, part I: critical appraisal of existing treatment guidelines and systematic review of current research evidence. *Osteoarthr Cartil* 2007; **15**: 981–1000.

3. Elias-Jones CJ, Farrow L, Reilly JH *et al.* Inflammation and neovascularization in hip impingement: not just wear and tear. *Am J Sports Med* 2015; **43**: 1875–81.

4. Hoaglund FT, Steinbach LS. Primary osteoarthritis of the hip: etiology and epidemiology. *Jaaos* 2001; **9**: 320–7.

5. Collins AT, Kulvaranon M, Spritzer CE *et al.* The influence of obesity and meniscal coverage on in vivo tibial cartilage thickness and strain. *Orthop J Sports Med* 2020; **8**: 2325967120964468.

6. Liu B, Lad NK, Collins AT *et al.* In vivo tibial cartilage strains in regions of cartilage-to-cartilage contact and cartilage-to-meniscus contact in response to walking. *Am J Sports Med* 2017; **45**: 2817–23.

7. Liao TC, Samaan MA, Popovic T *et al.* Abnormal joint loading during gait in persons with hip osteoarthritis is associated with symptoms and cartilage lesions. *J Orthop Sports Phys Ther* 2019; **49**: 917–24.

8. Hortobágyi T, Garry J, Holbert D *et al.* Aberrations in the control of quadriceps muscle force in patients with knee osteoarthritis. *Arth Care & Res* 2004; **51**: 562–9.

9. Howell G, Biggs R, Bourne R. Prevalence of abductor mechanism tears of the hips in patients with osteoarthritis. *J Arthrop* 2001; **16**: 121–3.

10. Meknas K, Johansen O, Steigen SE *et al.* Could tendinosis be involved in osteoarthritis? *Scand J Med Sci Sports* 2012; **22**: 627–34.

11. Domb BG, Botser I, Giordano BD. Outcomes of endoscopic gluteus medius repair with minimum 2-year follow-up. *Am J Sports Med* 2013; **41**: 988–97.

12. Pascual-Garrido C, Guilak F, Rai MF *et al.* Canine hip dysplasia: a natural animal model for human developmental dysplasia of the hip. *J Orthop Res* 2018; **36**: 1807–17.

13. Little D, Johnson S, Hash J *et al.* Functional outcome measures in a surgical model of hip osteoarthritis in dogs. *J Exp Orthop* 2016; **3**: 1–16.

14. Jónasson PS, Ekström L, Swärd A *et al.* Strength of the porcine proximal femoral epiphyseal plate: the effect of different loading directions and the role of the perichondrial fibrocartilaginous complex and epiphyseal tubercle–an experimental biomechanical study. *J Exp Orthop* 2014; **1**: 1–9.

15. Siebenrock KA, Fiechter R, Tannast M *et al.* Experimentally induced cam impingement in the sheep hip. *J Orthop Res* 2013; **31**: 580–7.

16. Pawaskar SS, Grosland NM, Ingham E *et al.* Hemiarthroplasty of hip joint: an experimental validation using porcine acetabulum. *J Biomech* 2011; **44**: 1536–42.

17. Teeple E, Jay GD, Elsaid KA *et al.* Animal models of osteoarthritis: challenges of model selection and analysis. *AAPS J* 2013; **15**: 438–46.

18. Gregory MH, Capito N, Kuroki K *et al.* A review of translational animal models for knee osteoarthritis. *Arthritis* 2012; **2012**: 764621.

19. Oláh T, Michaelis JC, Cai X *et al.* Comparative anatomy and morphology of the knee in translational models for articular cartilage disorders. Part II: small animals. *Ann Anat* 2021; **234**: 151630.

20. Killian ML, Locke RC, James MG *et al.* Novel model for the induction of postnatal murine hip deformity. *J Orthop Res* 2019; **37**: 151–60.

21. Wu CL, Jain D, McNeill JN *et al.* Dietary fatty acid content regulates wound repair and the pathogenesis of osteoarthritis following joint injury. *Ann Rheum Dis* 2015; **74**: 2076–83.

22. Jensen EC. Quantitative analysis of histological staining and fluorescence using ImageJ. *Anat Rec* 2013; **296**: 378–81.

23. Schmitz N, Laverty S, Kraus VB *et al.* Basic methods in histopathology of joint tissues. *Osteoarthr Cartil* 2010; **18**: S113–6.

24. Cole HA, Yuasa M, Hawley G *et al.* Differential development of the distal and proximal femoral epiphysis and physis in mice. *Bone* 2013; **52**: 337–46.

25. Wang M, Sampson ER, Jin H *et al.* MMP13 is a critical target gene during the progression of osteoarthritis. *Arthritis Res Ther* 2013; **15**: 1–11.

26. Shen J, Li J, Wang B *et al.* Deletion of the transforming growth factor β receptor type II gene in articular chondrocytes leads to a progressive osteoarthritis-like phenotype in mice. *Arthritis Rheum* 2013; **65**: 3107–19.

27. Roach HI, Yamada N, Cheung KS *et al.* Association between the abnormal expression of matrix-degrading enzymes by human osteoarthritic chondrocytes and demethylation of specific CpG sites in the promoter regions. *Arthritis Rheum* 2005; **52**: 3110–24.

28. Kawarai Y, Orita S, Nakamura J *et al.* Changes in proinflammatory cytokines, neuropeptides, and microglia in an animal model of monosodium iodoacetate-induced hip osteoarthritis. *J Orthop Res* 2018; **36**: 2978–86.

29. Ford CA, Nowlan NC, Thomopoulos S *et al.* Effects of imbalanced muscle loading on hip joint development and maturation. *J Orthop Res* 2017; **35**: 1128–36.

30. Draovitch P, Edelstein J, Kelly BT. The layer concept: utilization in determining the pain generators, pathology and how structure determines treatment. *Curr Rev Musculoskelet Med* 2012; **5**: 1–8.

31. Bunker TD, Esler CN, Leach WJ. Rotator-cuff tear of the hip. *J Bone Joint Surg Br* 1997; **79**: 618–20.

32. Kagan A 2nd. Rotator cuff tears of the hip. *Clin Orthop Relat Res* 1999; **368**: 135–40.

33. Hurley MV. The role of muscle weakness in the pathogenesis of osteoarthritis. *Rheum Dis Clin North Am* 1999; **25**: 283–98.

34. Herzog W, Longino D. The role of muscles in joint degeneration and osteoarthritis. *J Biomech* 2007; **40**: S54–S63.

35. Kingzett-Taylor A, Tirman PF, Feller J *et al.* Tendinosis and tears of gluteus medius and minimus muscles as a cause of hip pain: MR imaging findings. *AJR Am J Roentgenol* 1999; **173**: 1123–6.

36. Fang H, Beier F. Mouse models of osteoarthritis: modelling risk factors and assessing outcomes. *Nat Rev Rheum* 2014; **10**: 413–21.

37. Iidaka T, Muraki S, Oka H *et al.* Incidence rate and risk factors for radiographic hip osteoarthritis in Japanese men and women: a 10-year follow-up of the ROAD study. *Osteoarthr Cartil* 2020; **28**: 182–8.

38. Guillemin F, Rat AC, Mazieres B *et al.* Prevalence of symptomatic hip and knee osteoarthritis: a two-phase population-based survey. *Osteoarthr Cartil* 2011; **19**: 1314–22.

39. Prieto-Alhambra D, Judge A, Javaid MK *et al.* Incidence and risk factors for clinically diagnosed knee, hip and hand osteoarthritis: influences of age, gender and osteoarthritis affecting other joints. *Ann Rheum Dis* 2014; **73**: 1659–64.

40. Nepple JJ, Thomason KM, An TW *et al.* What is the utility of biomarkers for assessing the pathophysiology of hip osteoarthritis? A systematic review. *Clin Orthop Relat Res* 2015; **473**: 1683–701.